REPORT DOCUMENTATION PAGE

Form Approved

OMB No. 0704-0188

The public reporting burden for this collection of information is estimated to average 1 hour per response, including the time for reviewing instructions, searching existing data sources, gathering and maintaining the data needed, and completing and reviewing the collection of information. Send comments regarding this burden estimate or any other aspect of this collection of information, including suggestions for reducing the burden, to Department of Defense, Washington Headquarters Services, Directorate for Information Operations and Reports (0704-0188), 1215 Jefferson Davis Highway, Suite 1204, Arlington, VA 22202-4302. Respondents should be aware that notwithstanding any other provision of law, no person shall be subject to any penalty for failing to comply with a collection of information if it does not display a currently valid OMB control number.
PLEASE DO NOT RETURN YOUR FORM TO THE ABOVE ADDRESS.

1. REPORT DATE *(DD-MM-YYYY)*	2. REPORT TYPE	3. DATES COVERED *(From - To)*
30-09-2015	Final	25 Apr 2013 – 24 Apr 2015

4. TITLE AND SUBTITLE

Understanding of Materials State and its Degradation using Non-Linear Ultrasound Approaches for Lamb Wave Propagation

5a. CONTRACT NUMBER
FA2386-13-1-4001

5b. GRANT NUMBER
Grant 13RSZ070_134001

5c. PROGRAM ELEMENT NUMBER
61102F

6. AUTHOR(S)

Prof Krishnan Balasubramaniam

5d. PROJECT NUMBER

5e. TASK NUMBER

5f. WORK UNIT NUMBER

7. PERFORMING ORGANIZATION NAME(S) AND ADDRESS(ES)
IIT Madras
Center for Non Destructive Evaluation
Chennai 600036
India

8. PERFORMING ORGANIZATION REPORT NUMBER
N/A

9. SPONSORING/MONITORING AGENCY NAME(S) AND ADDRESS(ES)

AOARD
UNIT 45002
APO AP 96338-5002

10. SPONSOR/MONITOR'S ACRONYM(S)
AFRL/AFOSR/IOA(AOARD)

11. SPONSOR/MONITOR'S REPORT NUMBER(S)
13RSZ070_134001

12. DISTRIBUTION/AVAILABILITY STATEMENT

Distribution Code A: Approved for public release, distribution is unlimited.

13. SUPPLEMENTARY NOTES

14. ABSTRACT This research work was a continuation effort on earlier work efforts focused on the development of better understanding of non-linear ultrasonic methods for quantitative materials state evaluation and characterization of damage in metallic alloys. In this work, the Non-linear ultrasonic (NLU) method using guided Lamb modes was explored. Creep and associated damage mechanisms were simulated on metallic alloys of steel using standard test coupons that were subjected to different tempering temperatures. The results show that the Lamb wave NLU method can distinguish the different regions of damage. The improved understanding of the non-linear ultrasound is anticipated to lead to new measurement techniques with applications in the area of vehicle health monitoring, nondestructive testing, and monitoring of manufacturing processes.

15. SUBJECT TERMS

nondestructive evaluation, nonlinear ultrasonics, ultrasonics

16. SECURITY CLASSIFICATION OF:			17. LIMITATION OF ABSTRACT	18. NUMBER OF PAGES	19a. NAME OF RESPONSIBLE PERSON
a. REPORT	b. ABSTRACT	c. THIS PAGE			David Hopper, Lt Col, USAF, Ph.D.
U	U	U	SAR	26	19b. TELEPHONE NUMBER *(Include area code)* +81-42-511-2000

Final Report for AOARD Grant AOARD FA2386-13-1-4001

"**Research Title**" "Understanding of Materials State and its Degradation using Non-Linear Ultrasound Approaches for Lamb Wave Propagation"

Date: 31st May 2015

Name of Principal Investigators (PI and Co-PIs): Krishnan Balasubramaniam

- e-mail address : balas@iitm.ac.in
- Institution : Indian Institute of Technology Madras
- Mailing Address : MDS 301, Department of Mechanical Engineering, IIT Campus, Chennia INDIA 600036
- Phone : +91-44-2257-4662
- Fax : +91-44-2257-0545

Period of Performance: 04/25/2013– 04/24/2015

Abstract: Short summary of most important research results that explain why the work was done, what was accomplished, and how it pushed scientific frontiers or advanced the field. This summary will be used for archival purposes and will be added to a searchable DoD database.

This research work was a continuation effort on earlier work efforts and the overall program focuses on the development of new explorations towards the development of better understanding of non-linear ultrasonic methods for the quantitative materials state evaluation and characterization of damage in metallic alloys. In this work, the Non-linear ultrasonic method using guided Lamb modes have been explored. The creep and associated damage mechanism were simulated on metallic alloys of steel using standard test coupons that were subjected to different tempering temperatures. The results show that the Lamb wave NLU method can distinguish the different regions of damage. The improved understanding of the non-linear ultrasound is anticipated to lead to new measurement techniques that have applications in the area of vehicle health monitoring, nondestructive testing, and process monitoring of manufacturing processes

Introduction:

The work was divided into (a) Test coupon preparation and damage simulation in laboratory conditions, (b) Experimental apparatus development and choice of appropriate modes, and (c) Experimental tasks that develop a relationship between damage progression in metals and the Non-Linear Ultrasonic parameters using Lamb modes.

Theoretical Development: The details are provided in APPENDIX A.

Experiment: The details are provided in APPENDIX A.

Results and Discussion: The significant results are listed below:

1. The Lamb wave based Non-Linear ultrasonic measurements are feasible on test coupons if the pairs of Lamb modes are selected appropriately.
1. Non-Linear ultrasonic measurements can be correlated with damage in metallic alloys. It was observed that the Normalized non-linear ultrasonic Lamb mode parameter (β) was observed to be highly dependent on the

Distribution Code A: Approved for public release, distribution is unlimited.

precipitate-matrix coherency strains generated during different tempering temperatures.

List of Publications and Significant Collaborations that resulted from your AOARD supported project: In standard format showing authors, title, journal, issue, pages, and date, for each category list the following:

a) papers published in peer-reviewed journals, NONE
b) papers published in peer-reviewed conference proceedings, NONE
c) papers published in non-peer-reviewed journals and conference proceedings, NONE
d) conference presentations without papers, NONE
e) manuscripts submitted but not yet published, NONE
f) provide a list any interactions with industry or with Air Force Research Laboratory scientists or significant collaborations that resulted from this work. NONE

Attachments: Publications a), b) and c) listed above if possible.

DD882: Attached

APPENDIX A

Lamb Wave Based Non-Linear Ultrasound for Damage Detection

(i) Problem Definition:

Structural metals are subject to aging from fatigue, creep, corrosion, and their combination. Exposure to elevated temperatures promotes creep and in-service degradation with creep is one of the most critical factors determining the structural integrity of components at elevated temperatures in power plants, chemical plants, and oil refineries. Presently for saving energy and to meet recent regulations of CO_2 emissions, as well as to improve thermal efficiency, the steam pressures and operating temperatures have been increased, resulting in accelerated material-degradation. So there is an increasing concern regarding the safety of power-plant components used in high temperature environment. Assessment of the state of creep damage is, therefore, important to ensure safe operation, to predict remaining life, and to promote life-extension programs.

Creep damage involves the nucleation and growth of cavities at the grain boundaries, their subsequent linkage to form micro-cracks, and the propagation of micro-cracks until failure. During this process, the precipitation of the second phase particles such as carbides and inter-metallic compounds is accompanied. For assessing this damage, nondestructive techniques have long been desired. Ultrasonic and electro-magnetic based techniques have been explored by various researchers to assess creep damage. However, there is no established NDE technique that enables evaluation of the present state of materials and predicts their remaining life. Conventional ultrasonic methods and all other conventional NDT techniques are all point-to-point inspection methods that are only the part under the transducer can be inspected. So conventional NDT techniques are not desirable for inspection of tubes and pipes. On the other hand, guided wave ultrasonic technique has been introduced as a technique for long range pipe inspection and evaluation of inaccessible parts. This guided wave ultrasonic has two distinguishable advantages: (i) it can propagate along the pipe for long distance without much energy attenuation, so it can be used for long-range inspection; (ii) this type of waves vibrate in the inner, center, and outer part of the pipe, thus 100% pipe inspection can be achieved.

Background:

Nondestructive Technique for creep damage evaluation for in-service components requires continuous monitoring or periodic inspection of the actual components to identify any defects such as cracks or voids. Among those techniques, ultrasonic has a long success history in many NDE applications both in lab conditions and in the field [1]. Most of the works co-relate the ultrasonic velocity distribution with the porosities formed during creep damage. Stigh [2] showed relations between the ultrasonic velocity and the ultimate strength

of crept samples, which might be used to assess the load carrying capacity of a structural element. The material properties (density, elastic moduli, electrical resistivity etc.) are changed due to the formation of porosity during creep damage of various power-plant components. So the potential of several NDT techniques for the detection of creep cavities are discussed by several authors. H. Willems and G. Dobmann [3] traced the changes in density and elastic moduli by ultrasonic velocity measurement and they made a theoretical estimation which showed a good agreement with experimental results under laboratory conditions. T. Morishita *et al.* [4] measured the ultrasonic velocities and porosity for pure copper samples subjected to the intergranular creep process. They studied a double composite model implied by photomicrographic observations and calculated the transversely isotropic effective stiffness using this micromechanical modelling. H. Jeong & D H Kim [5] investigated the creep voids-ultrasonic velocity relationships on a series of crept copper samples and a progressive damage model was developed considering the anisotropic behaviour of the material. B. J. Kim *et al.* [6] studied the ultrasonic backscattering signal to evaluate the creep-fatigue strength and the creep-fatigue life of high-pressure vessels at high temperature in a power-plant. The relationships between the ultrasonic bulk-waves parameters, RMS level of backscattering signals, and the area fraction of the cavity in the creep-fatigue zone were investigated by them to evaluate the life-time of the damaged P92 specimens. Very recently some advanced ultrasonic techniques have also been used to assess the creep damage. Phased-Array Ultrasonic [7] is being used to detect any flaw or defects present in the welded as well as HAZ region. Nonlinear Ultrasonic (NLU) is also now used to characterise the creep damage. Sony Baby *et al*. used the NLU technique to show a good agreement between experimental results and the metallographic studies for titanium alloy [8]. Co-relation between the micro-void concentrations caused by creep damage, dislocation morphologies and the NLU parameters were made by Valluri *et al.* and Balasubramaniam *et al.* [9, 10]. Guided wave ultrasonic technique has been used for pipe inspection for corrosion damage, structural health monitoring, measurement of wall thinning in pipes, tubes and shells due to various type of damages, etc. [11-13]. Nonlinear guided wave ultrasonic has been studied by Jacobs for various types of damages [15-17].

Sample Preparation:

Machining was done for making creep flat specimens from Cr-Mo steel as well as IN-718 as per the drawing given in figure-1. Cr-Mo Steel:: The chemical compositions of the Cr-Mo steel are given below (Table-1):

Distribution Code A: Approved for public release, distribution is unlimited.

Table-1:

Radicals (%)	C	Si	Mn	P	S	Ni	Cr	Mo	W
	0.057	0.277	0.408	0.023	0.005	0.08	8.57	0.89	0.015

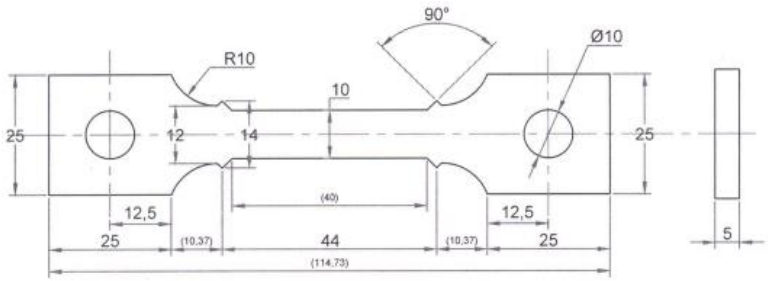

Fig-1: Drawing of a flat Creep sample (All dimensions in mm)

Microstructural Analysis:

The received plate of 9Cr-1Mo steel was solution annealed. The heat-treatment was done at 1050^0C for 2 hrs and air-cooling followed by tempering at 750^0C for 1hr and air-cooled. Figure-2 (a) & (b) show the optical microstructure of the solution annealed 9Cr-1Mo sample which is tempered martensitic structure.

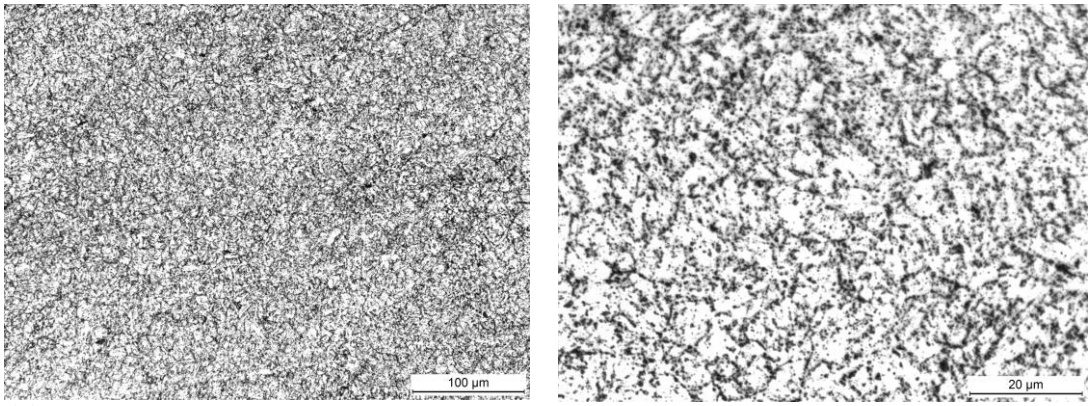

(a) *(b)*

Fig.-2(a) & (b): Showing the optical microstructure at different magnifications

Figures-3 show the dislocation morphologies and various precipitates of the solution annealed 9Cr-1Mo sample using transmission electron microscope.

Distribution Code A: Approved for public release, distribution is unlimited.

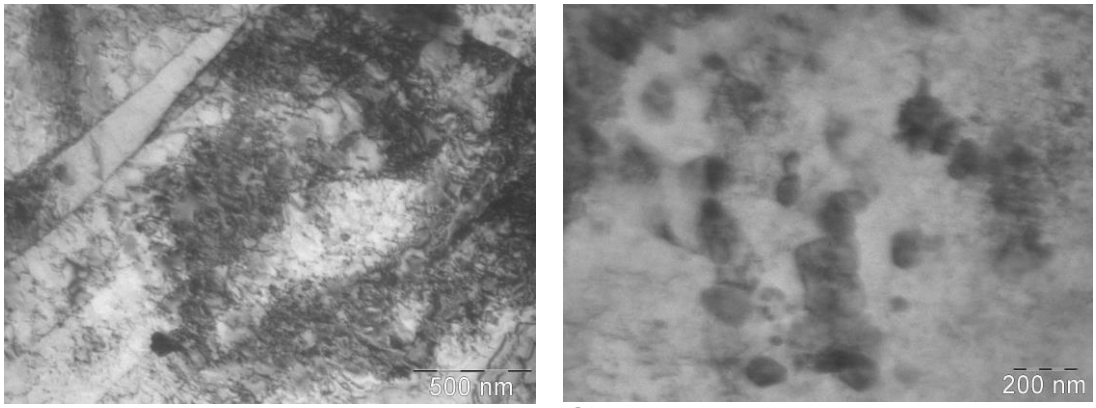

(a) *(b)*

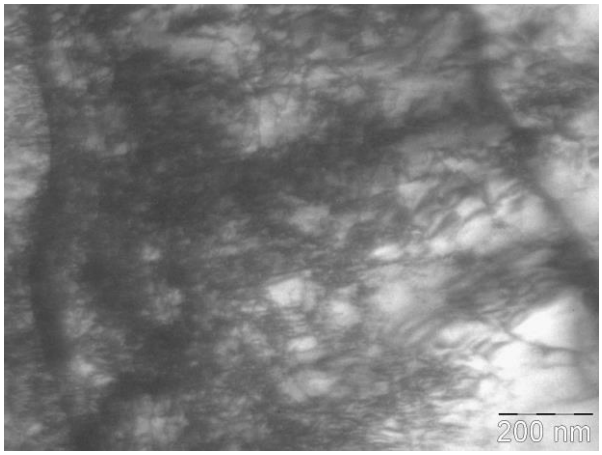

(c)

Fig.-3: TEM micrograph of the solution-annealed 9Cr-1Mo steel

Prior austenitic grain boundary can be seen in fig.-3(a) along-with elongated grains. Lots of dislocations tumble in the microstructure. Presence of carbides in the initial microstructure is presented in fig.-3(b). Fig.-3(c) also shows the tempered martensite within the prior austenitic grain boundary and the orientations of the martensitic structure are almost same within the grain boundary.

Mechanical Evaluation:

Fig.-4 shows the tensile curve of 9Cr-1Mo steel at room temperature and at 600^0C at which creep testing has been going on. The calculated yield stress, UTS and the elongation at room temperature as well as at 600^0C are given below in table-2.

Distribution Code A: Approved for public release, distribution is unlimited.

Table-2:

Temperature	Yield Stress (corresponding to 0.2% strain)	UTS	Elongation (Based on position data with gage length 40 mm)
Room	644.168 MPa	871.32 MPa	15.2 %
600^0C	407.86 MPa	480 MPa	22.25 %

The hardness values of the solution annealed sample (Taken at 5-positions) are 277.6HV, 283.1 HV, 279.0 HV, 280.3 HV and 280.3 HV using 30 kg load.

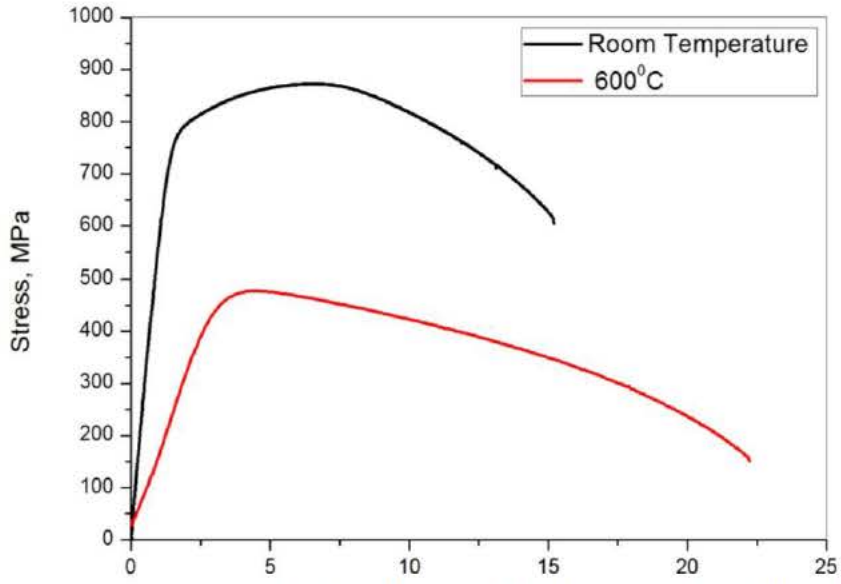

Fig.-4: Tensile curve of solution annealed 9Cr-1Mo steel

Creep test has been going on of 9Cr-1Mo steel at 600^0C under 140 MPa to evaluate the rupture life as well as the creep strain.

Nonlinear Ultrasonic using Ultrasonic Lamb Waves:

The disperse curves of phase velocity as well as group velocity for 5mm thickness steel plate are shown in figure-5 & 6. At first, simulation is done for excitation of S_0 mode using 250 kHz. The material is assumed as linear, isotropic and homogeneous. So, the FFT of the received simulated signal shows the presence of only 250 kHz without any higher harmonics

Distribution Code A: Approved for public release, distribution is unlimited.

as no non-linearity in the material is assumed. The finite element simulation was done in ABAQUS [18] using plane strain elements of 4-node bi-linear, hour-glass, reduced integration type element both for wedge as well as plate. For getting proper frequency components, at least 10 nodes per wave-length were taken [19].

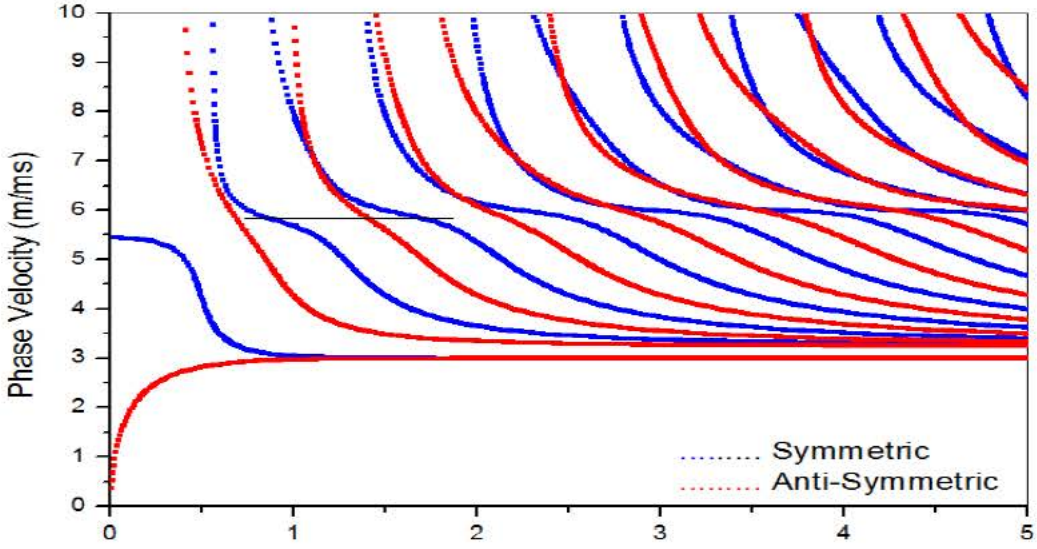

Fig.-5: Disperse Curve showing Phase velocity variation for 5mm thick steel plate

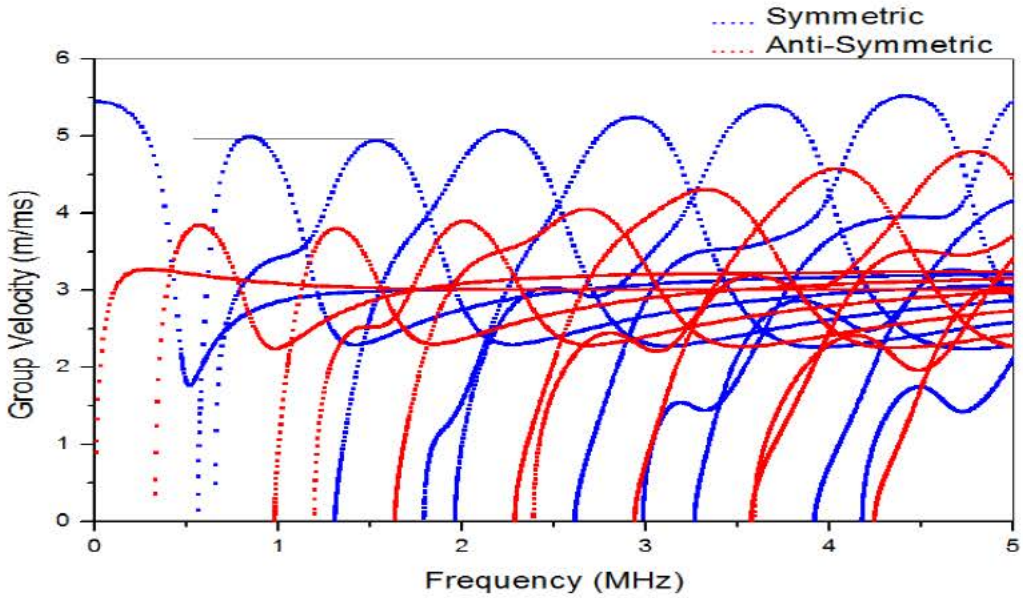

Fig.-6: Disperse Curve showing Group velocity variation for 5mm thick steel plate

The excitation frequency of 250 KHz tone-burst Hanning windowed signal with 5-cycles is

Distribution Code A: Approved for public release, distribution is unlimited.

applied on the wedge assuming the crystal diameter as 10 mm. Fig.-7 shows the excitation signal and corresponding FFT of that signal.

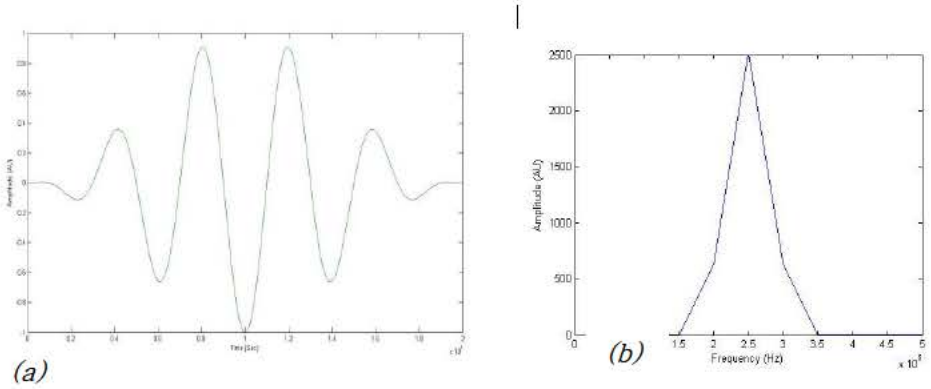

Fig.-7: Input signal used for simulation (a) Time domain (b) Frequency domain

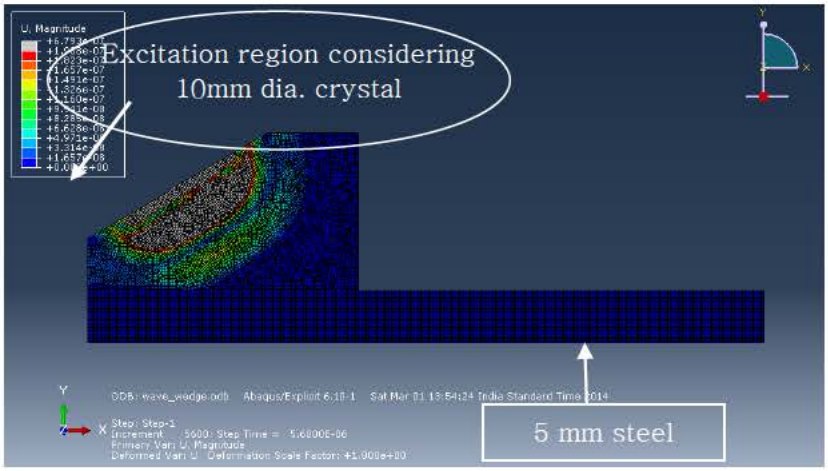

(a)

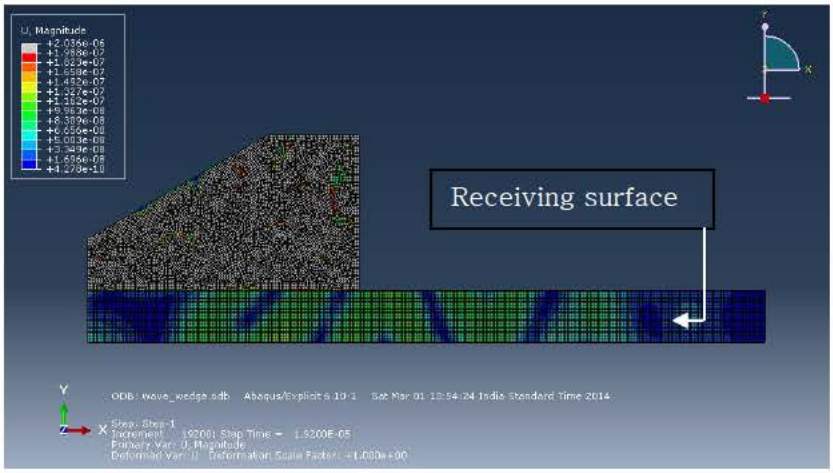

(b)

Fig.-8(a & b): Lamb Wave propagation through 5 mm steel plate

Distribution Code A: Approved for public release, distribution is unlimited.

The received signal with its FFT at the receiving surface is shown in figure-9. It can be seen that only 0.25 MHz frequency has been generated. The current simulation was carried out at a relatively lower excitation frequency of 250 kHz where no situation of identical group and phase velocity exists [20]. At certain high excitation frequencies, higher harmonics can be seen in the result when the condition of identical group and phase velocities exists for the harmonics [21].

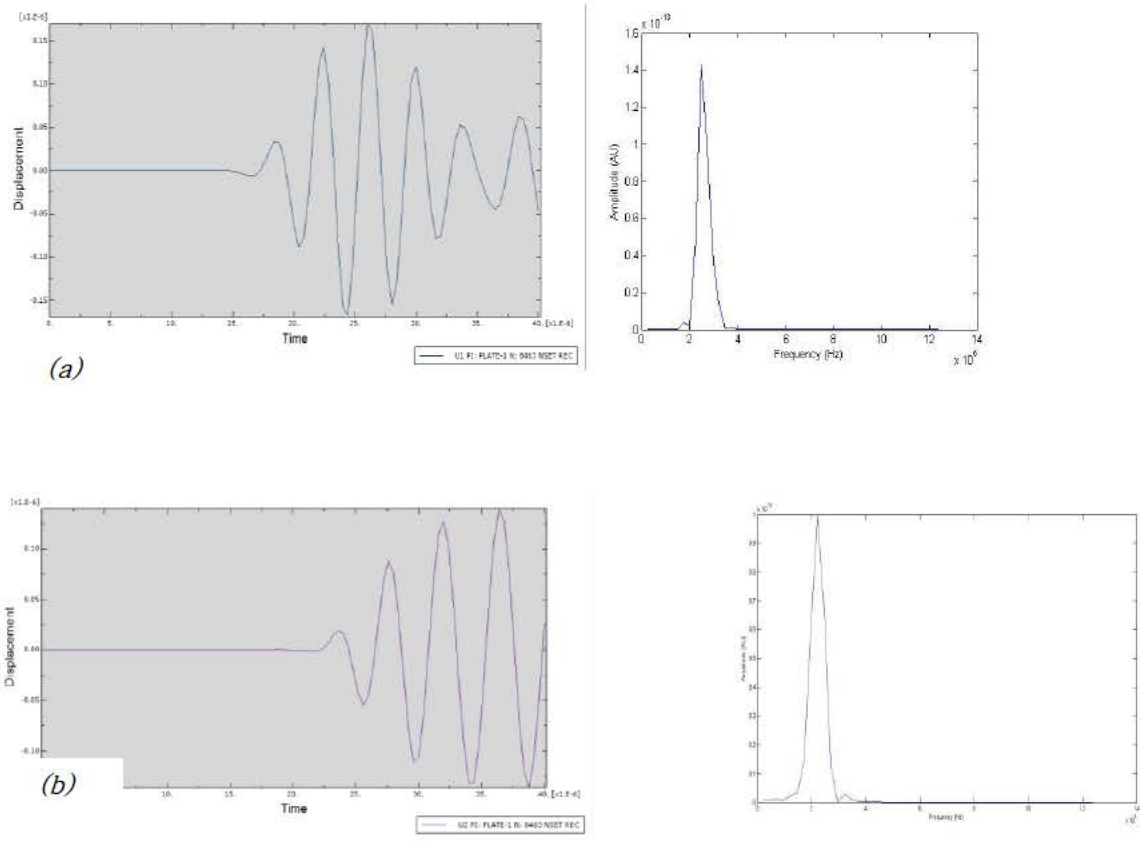

Fig.-9: (a) The received simulated U1 displacement and it's FFT
(b)The received simulated U2 displacement and it's FFT

Distribution Code A: Approved for public release, distribution is unlimited.

Generation of lamb wave by non collinear wave mixing [22-24]:

Simulation of generation of guided wave by wave mixing of two non collinear waves has been going on. The schematic diagram which is adapted for this technique is shown in fig. - 10.

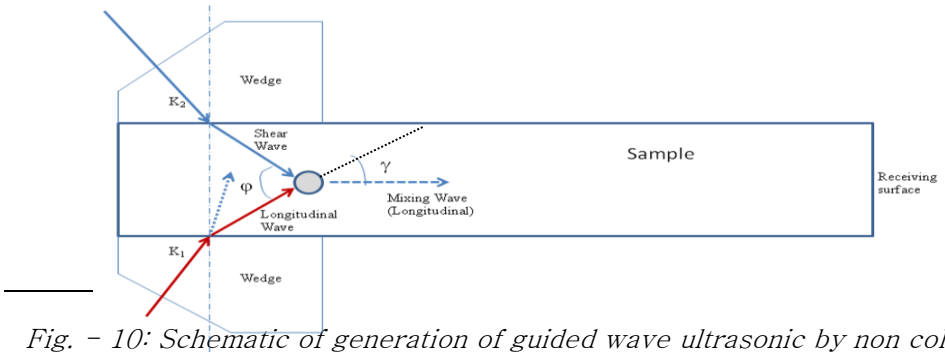

Fig. – 10: Schematic of generation of guided wave ultrasonic by non collinear ultrasonic

where,

$$\tan\gamma = \frac{a\sin\varphi}{c + a\cos\varphi}$$

$$a = \frac{\omega_2}{\omega_1} \quad \text{and} \quad c = \frac{c_t}{c_l}$$

C_t = Transverse velocity of ultrasonic bulk wave

C_l = Longitudinal velocity of ultrasonic bulk wave

Brief literature review:

Nonlinear ultrasonic technique has been emerging as potential non-destructive tool for evaluating plastic deformation in a material. Initially sinusoidal ultrasonic wave gets distorted and generates higher order harmonics, when propagates through nonlinear or anharmonic materials. The quantitative measurement of this distortion is given by nonlinear acoustic parameter

$$\beta = \frac{8A_1}{k^2A_2^2x}$$

where A_1 and A_2 are the displacement amplitudes of the first and second harmonics respectively, k is the wave vector and x is the propagation distance. The generation of higher order harmonics is related to nonlinear elastic properties of the materials. These nonlinear

Distribution Code A: Approved for public release, distribution is unlimited.

elastic properties are much more sensitive to microstructural changes than linear elastic properties [25]. The variations of harmonic generation can be related to the microstructural changes in materials. Cantrell *et. al.* [26] demonstrated the variation of harmonic generation during aging in precipitation hardened Al2014 hardened alloys and showed that acoustic nonlinear parameter in a heat-treatable alloy could provide quantitative information about the kinetics of precipitation nucleation and growth in such alloys. Hurley *et. al.* [27] showed the variation of β in quenched martensitic steel. β was found to increase monotonically with carbon content over the range of 0.10-0.40 mass% C. Attempts have also been made by several researchers to characterise the material degradation by measuring the amount of harmonics generated which confirm that the harmonic generation technique could be the potential tool for material characterisation [28-30]. All these works are based on bulk longitudinal waves for the generation of harmonics i.e. point-to-point measurement. There are also some experimental investigations in which Rayleigh surface waves are used for assessing the accumulated materials damage by acoustic nonlinearity [31-33].

In present investigation, guided Lamb wave is used to evaluate the nonlinearity of material during tempering. The main advantage of using guided wave (such as Lamb wave used in this work) is that, it can be used for long range inspection of any plate or shell type structures and only one sided access using pitch-catch configuration is required. But, due to the inherent multi-mode and dispersive nature of Lamb wave, it's difficult to accurately extract the second harmonic component. Deng *et. al.* [34] carried out experiments on nonlinear Lamb wave for cyclic plastic damage in aluminium. They used stress wave factor (SWF) as a nonlinearity acoustic parameter which was defined as absolute magnitude of the second harmonic signal integrated over a certain frequency range. According to this work, SWF decreased monotonically with fatigue cycles, which was contrary to the work done by other researchers using longitudinal bulk waves [28-30, 35]. Bermes *et. al.* [36] used nonlinear Lamb waves to detect plasticity driven damage in material. In their work, hybrid wedge generation and laser interferometric detection were used to measure the material nonlinearity parameters. Evaluations of material damage due to plastic deformation have also been studied by various researchers [37-40]. All these works show the cumulative growth of second harmonic component with propagation distances and material degradation. Very few attempts are there in evaluating thermal degradation in structural materials using the nonlinear effect of Lamb wave propagation [41-44]. A "mountain shape" change in the second harmonic component of Lamb wave with thermal degradation was observed in FeCrNi alloy steels [41]. Cumulative second harmonic analysis of ultrasonic Lamb wave was

Distribution Code A: Approved for public release, distribution is unlimited.

performed to study the precipitation kinetics and micro-void initiation of modified HP austenite steel during aging [42]. Initial increase in normalized acoustic nonlinearity parameter due to fine precipitates followed by decrease due to precipitate coarsening and micro-void formation was observed in this study. Very recently effect of precipitate-dislocation interactions during creep on Lamb wave propagation was studied in Ti-60 plates [43-44].

The objective of proposed work was to characterize the structural change of modified 9Cr-1Mo steel with tempering temperatures. Experiments were designed to introduce controlled level of measurable changes at different process parameters. The behaviour of β parameter was evaluated for each condition. Finally, pre-dominant effect was identified in terms of microstructural characteristics influencing β parameter significantly.

2. Experimental Efforts on Lamb Wave Non-Linear Ultrasound

2.1 Specimen preparation and microstructures

The as-received plate was machined to make rectangular shape of dimensions ~100mm x 40mm x 2.5mm with an objective of studying the higher harmonic component induced in Lamb wave during tempering. The machined rectangular plates were solution annealed (SA) at the temperature of ~1080^0C for 2 hours and then air-cooled. Tempering was done at 6 different temperatures from 600^0C to 850^0C at 50^0C interval for 1.5 hrs, followed by furnace cooling. Evaluation of microstructure was done in analytical transmission electron microscope (TEM; Philips CM 200). Samples for TEM were prepared by conventional method with final thinning using a mixture of acetic:perchloric acid (9:1) at 10^oC and 35V.

2.2 Nonlinear Lamb wave measurement

Higher harmonic measurement was done using high voltage tone-burst signal of 5 cycles at exciting frequency of 2 MHz generated by high power pulser RAM 5000 from RITEC Inc. A centre frequency of 2.25 MHz narrowband transducer was used as transmitter and 5 MHz broadband transducer was used as receiver. Figure-11 shows the experimental set-up for the higher harmonic measurement using Lamb wave.

Distribution Code A: Approved for public release, distribution is unlimited.

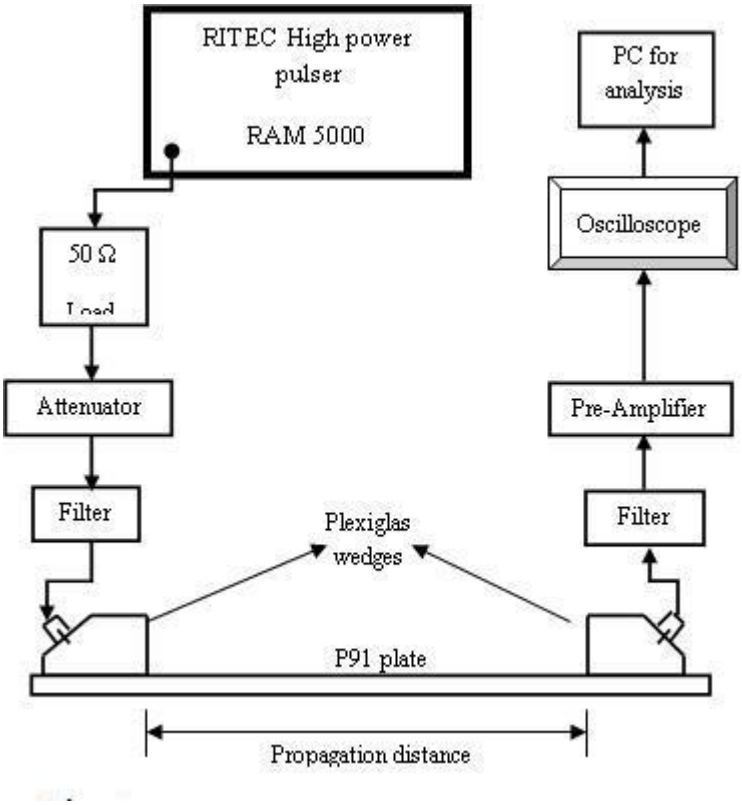

Fig. 11: Block diagram for nonlinear Lamb wave measurement.

Distribution Code A: Approved for public release, distribution is unlimited.

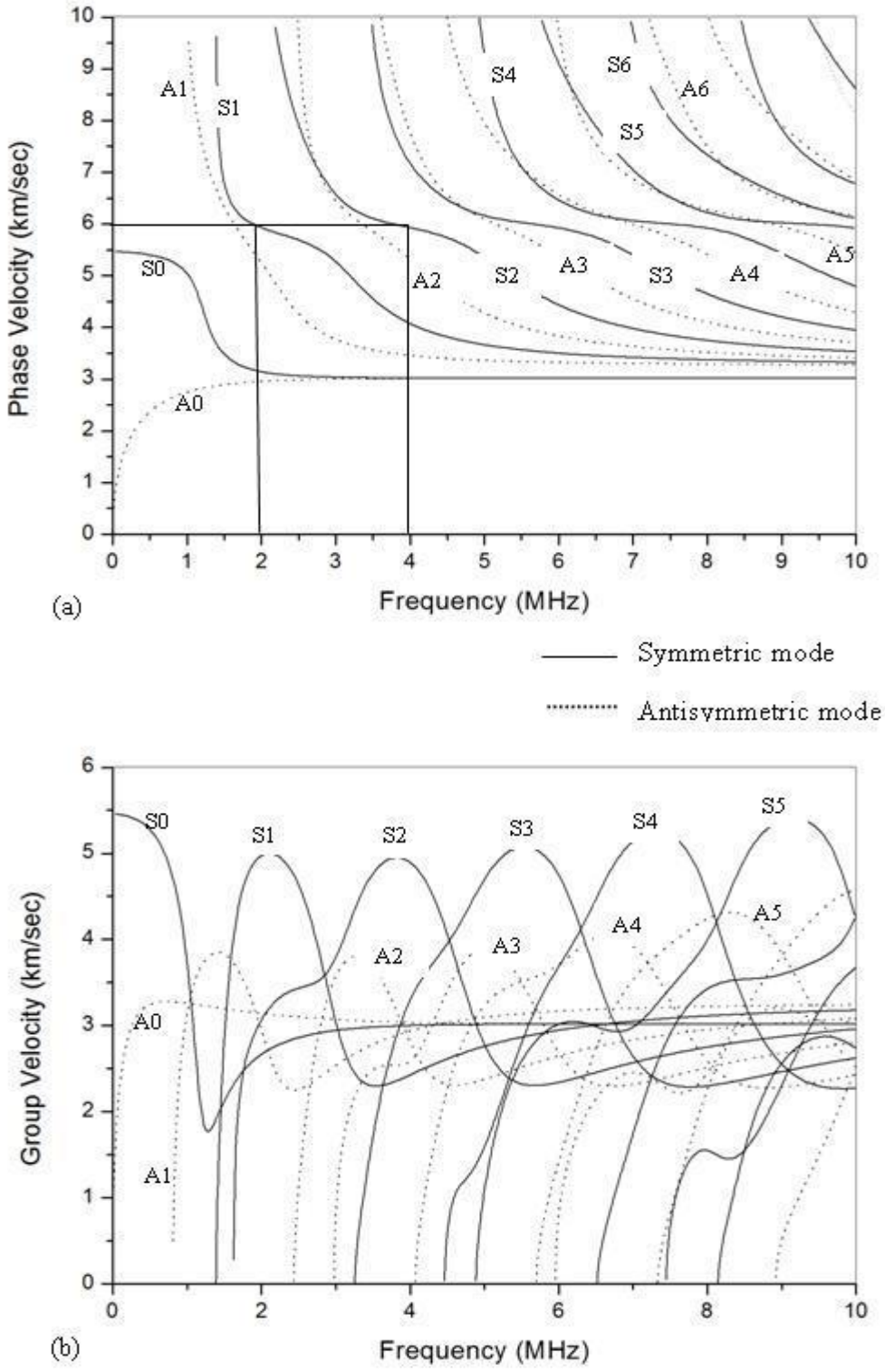

Fig. 12: Dispersion curves for 2.5 mm thick P91 steel plate: (a) phase velocity variation with frequency; and (b) group velocity variation with frequency.

Fig.12 shows the phase velocity and group velocity dispersion curves of Lamb waves for a 2.5 mm thick modified 9Cr-1Mo steel plate where S1 and S2 modes have been selected for higher harmonic measurement. These modes satisfied the conditions of phase velocity matching for excitation of cumulative second-harmonic of Lamb wave as well as group

Distribution Code A: Approved for public release, distribution is unlimited.

velocity matching for ensuring the transferred energy from the fundamental frequency to stay within the same wave packet [37-39, 45-47]. This synchronous Lamb wave mode pair (S1, S2) was excited and received using wedge (plexiglas made) transducers with an oblique angle of 27.7^0. The propagation distance within the material between transmitter and receiver was kept constant as ~80mm for all tempered specimens after adjusting the distance travelled by the wave in wedges.

A typical transient time-domain Lamb wave signal measured during this study from a tempered sample is shown in Fig.13. The signal shows the dispersive and multi-mode nature of Lamb waves. To determine the arrival times of the individual modes, suitable time-frequency analysis was performed on the signals. STFT (Short Time Fourier Transformation) was executed on the received Lamb wave signals for proper separation of various modes present in signal. The present work has followed the same analysis method as described by Bermes *et. al.* [36]. The fundamental and the second harmonic frequency components of the received signal are shown in Fig.14(a-b). The amplitude A_1 and A_2 were measured from these components and normalized β was calculated using the expression A_2/A_1^2.

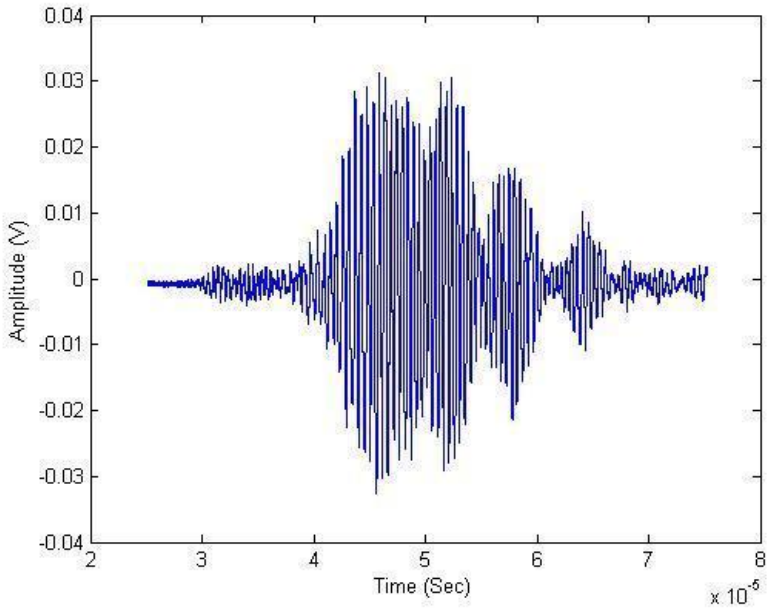

Fig 13: Typical multimode time-domain signal during nonlinear Lamb wave measurement.

Distribution Code A: Approved for public release, distribution is unlimited.

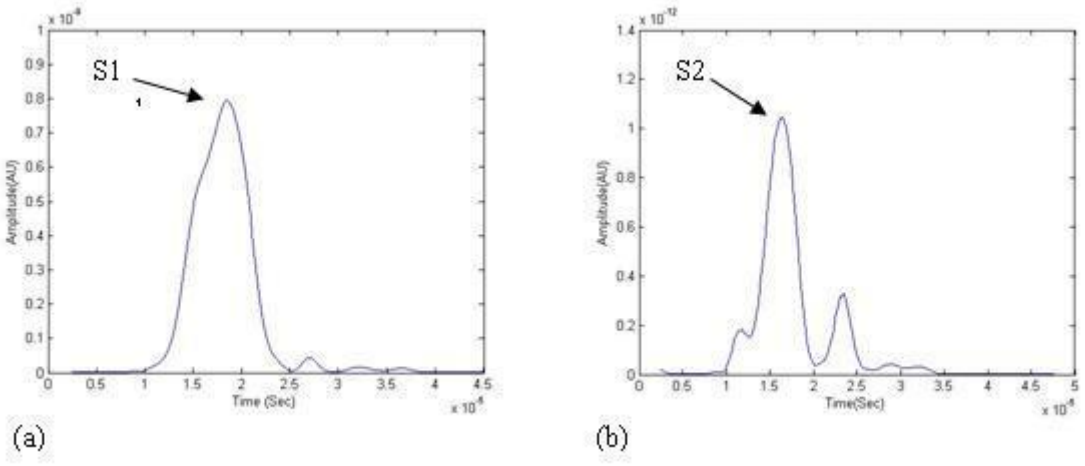

Fig 14: Time-frequency components of (a) S1 mode [2 MHz], (b) S2 mode [4 MHz].

2.3 Measurement of dislocation density by ultrasound

Influence of dislocations on the generation of higher harmonic component has been well established [48-52]. A relation between distribution of dislocations and β is there, where it is shown that $\beta \alpha NL^4\sigma$ where N = dislocation density, L= dislocation loop length and σ = applied or residual stress [48, 49]. So, measurement of dislocations is one of the important parameters to explain the change in β in de-generated materials. Till now, TEM and X-ray diffraction (XRD) are the two common techniques for measuring the dislocation density. TEM allows for a local measurement in a specially prepared sample that includes non-direct measurement of thickness for estimating the volume under observation. XRD technique though reflects a global characteristic, yet is limited to depth of penetration within the material under investigation. In this work, ultrasound was used to evaluate the dislocation density as discussed by N Mujica *et. al.* [53]. According to their work, it was seen that increase in dislocation density resulted in a decrease in shear wave velocities as given by eqn. (1).

$$\frac{\Delta v_T}{v_T} = -\frac{8}{5\pi^4}\frac{\mu b_s^2}{\Gamma_s}\Delta(n_s L_s^3) - \frac{4}{5\pi^4}\frac{\mu b_e^2}{\Gamma_e}\Delta(n_e L_e^3) \quad (1)$$

This equation links the relative change in shear wave velocity $\Delta v_T/v_T$ between two samples of a material that differ in dislocation density n, where n = number of dislocation segments of length L, b= Burgers vector, Γ = line tension per unit volume, μ = shear modulus and subscript e and s are related to edge and screw dislocations, respectively. Simplifying the

Distribution Code A: Approved for public release, distribution is unlimited.

expression [54] and assuming shear wave velocity is almost half of the longitudinal wave velocity the final relation will be:

$$\frac{\Delta v_T}{v_T} \equiv -\frac{8}{5\pi^4}\Delta(nL^3)$$

This formula provides a measure of the dimensionless quantity nL^3 and does not give an absolute measurement of dislocation density, but a measurement of the difference in dislocation density between two samples [53]. Shear wave velocity was measured using a 5 MHz PZT transducer by pulse-echo technique.

3. Results and Discussion

3.1. Variation of ultrasonic nonlinearity parameter

Heat-treatable metallic alloys are very much sensitive to precipitation, since they are generally strengthened as a result of nucleation and growth of precipitates that form during heat-treatment of materials. Precipitate has a definite lattice parameter that is different from that of matrix. If the lattice parameter of precipitate is denoted by a_p and a_m for matrix, then there will be a misfit which is a measure of lattice mismatch and is given as $\delta = (a_p - a_m)/a_m$. For one-to-one registry of atoms between precipitate and matrix then "coherency strains" are generated in the region around the interface [62]. Coherency strain may be given as $\varepsilon = 2(a_p-a_m)/(a_p+a_m)$.

The coherency strain causes the dislocations to bow during its movement over glide plane as shown in Fig.35 [63]. Assuming three precipitates are crudely collinear with a separation distance of L between two adjacent precipitates [64], it was shown by Hikata *et al.* [48] that normalized acoustic nonlinearity parameter ($\Delta\beta/\beta_0$) resulting from the application of a stress σ on a pinned dislocation segment of length 2L was

$$\frac{\Delta\beta}{\beta_0} = \frac{24}{5}\frac{\Omega\Lambda L^4 R^3 C_{11}^2}{\beta_0 G^3 b^2}|\sigma| \qquad \text{---------- (1)}$$

Distribution Code A: Approved for public release, distribution is unlimited.

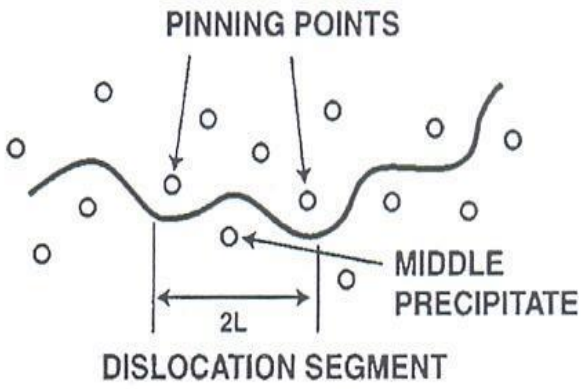

Fig. 15: Bowing (three-point bending) of dislocation segments on a matrix slip plane resulting from local precipitate-matrix coherency stress [63]; solid line and circles represent dislocation and precipitate respectively.

Where, $\Delta\beta = (\beta - \beta_0)$ = change in nonlinearity parameter and β_0 was the initial value; b = Burgers vector, Λ = dislocation density, C_{11} = second order elastic constant, G = shear modulus, R = Schmid or conversion factor associated with resolution of the longitudinal acoustic wave along the dislocation slip plane and Ω = conversion factor from shear strain to longitudinal strain. Considering dislocation line followed roughly the contour of the minimum interaction energy between adjacent precipitates, the radial stress in the matrix at a radius r from a spherical precipitate of radius r_1 embedded in a finite body was given by [65]

$$\sigma = -\frac{4G\delta r_1^3}{r^3} \qquad \text{---------- (2)}$$

From Eq. (1) and (2) for r = L/2, we get

$$\frac{\Delta\beta}{\beta_0} = 154\frac{\Omega\Lambda L R^3 C_{11}^2 |\delta| r_1^3}{\beta_0 G^2 b^2} \qquad \text{--------- (3)}$$

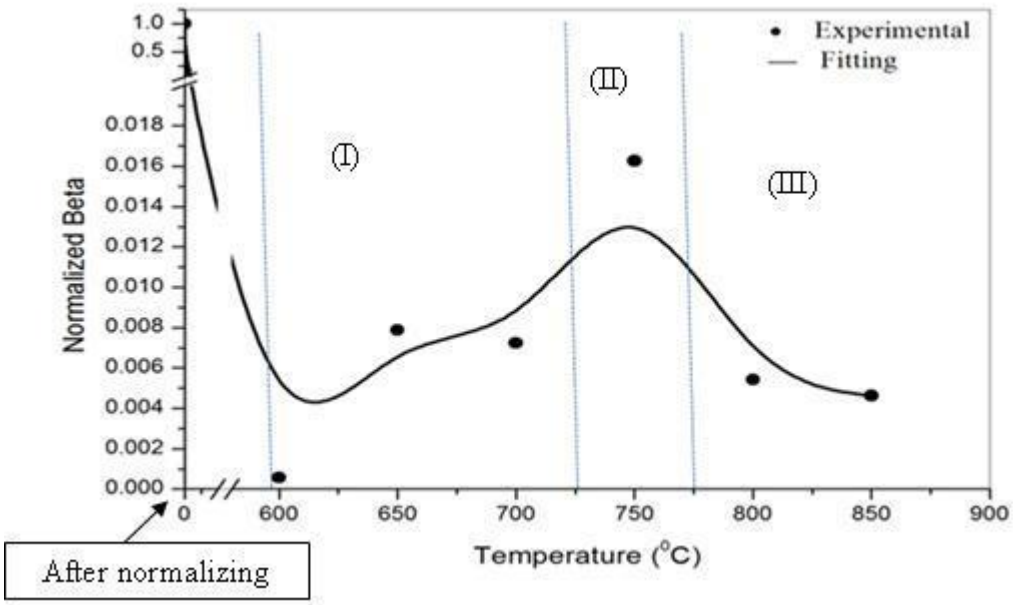

Fig. 16: Variation of ultrasonic nonlinearity parameter with tempering temperatures.

The variation of nonlinearity parameter using Lamb wave has been shown in Fig.16. This curve is showing the increase in normalized acoustic nonlinearity parameter from 600^0C, attains peak value at 750^0C and then decreases. Thus the curve may be divided into three regions.

Region-I:

Initial increase in normalized nonlinearity parameter from 600^0C in region-I was due to coherency strains associated with the nucleation of fine precipitates that impeded the dislocation motion resulting in increase of β (Eq.-3). In this stage, the material strength (flow stress) was increased as the dislocation motion was impeded by the fine MX type of precipitates and this resistance was increased due to increase in precipitate sizes within the coherency limit [62].

Region-II:

As the precipitate size increased with temperature and reached to a critical size at 750^0C, the generated coherency strain was maximum; so the control of flow stress shifted to the larger coherency strains that gave the optimum strength of the materials which in turn gave the maximum value of the acoustic nonlinearity parameter. In this case, the material strength was independent of precipitate size,

Distribution Code A: Approved for public release, distribution is unlimited.

since dislocations must penetrate this stress field (related to the corresponding coherency strain) before cutting through precipitate. Dislocation density was also reached to maximum value due to this higher coherency strain. According to Cantrell *et. al.* [62], this situation corresponds to the optimum heat treatment and maximum strength of the material.

Region-III:

Further growth of the precipitate sizes lead to "loss of coherency" and also loss of material strength. Following Eq.-3, Fig.16 showed the decrease of normalized β after 750^0C. Coarsening of the precipitates resulted in dissolving of the precipitates in the matrix and increases the inter-precipitate spacing which produces the dislocation mobility; so material strength further losses [62].

4. Conclusions:

From the studies conducted on the development of improved understanding on the use of Lamb Wave Non-linear Ultrasonic approach the following conclusions are derived:

2. Precipitation study of modified 9Cr-1Mo steel was done at various tempering temperatures by acoustic nonlinearity parameter (β) using Lamb wave.
3. Normalized β is seen to be highly dependent on the precipitate-matrix coherency strains generated during different tempering temperatures.
4. Maximum value of β was observed at 750^0C which indicates that 750^0C could be the optimum tempering temperature for this material where flow stress or material strength is maximum.

5. References:

[1] G. Sposito, C. Ward, P. Cawley, P.B.Nagy, & C. Scruby, "A review of non-destructive techniques for the detection of creep damage in power plant steels", *NDT&E International*, 2010; 43: 555-567.

[2] U. Stigh, "Influence of damage on ultrasonic velocity and strength - analysis & experiments", *Engineering Fracture Mechanics*, 1987; 28(1): 1-12.

[3] H. Willems, & G. Dobmann, "Early detection of creep damage by ultrasonic and electromagnetic techniques", *Nuclear Engineering and Design*, 1991; 128:139-149.

[4] T. Morishita, & M. Hirao, "creep damage modelling based on ultrasonic velocities in

Distribution Code A: Approved for public release, distribution is unlimited.

copper", *Int. J. Solids Structures*, 1997; 34(10): 1169-1182.

[5] H. Jeong, & D H kim, "A progressive damage model for ultrasonic velocity change caused by creep voids in copper", *Mat. Sc. and Eng. A*, 2002; 337:82-87.

[6] B J kim, H J Kim, & B S Lim, "Creep-fatigue damage and life prediction in P92 alloy by focussed ultrasonic measurements", *Met. and Mat. Int.*, 2008; 14(4): 391-395.

[7] M. Tabuchi, H. Hongo, Y Li, T Watanabe, & Y Takahashi, "Evaluation of microstructures and creep damage in the HAZ of P91 steel weldment", *J. of Pr. Vessel tech.*,2009; 131:021406-1.

[8] S Baby, B N kowmudi, C M Omprakash,D V V Satyanarayana, K Balasubramaniam, & V Kumar, "Creep damage assessment in titanium alloyusing a nonlinear ultrasonic technique",*Scripta Materialia*, 2008; 59:818-821.

[9] S Valluri, K Balasubramaniam, & R V prakash, "Creep damage characterisation using nonlinear ultrasonic techniques", *Acta Materialia*, 2010; 58:2079-2090.

[10] K. Balasubramaniam, J S Valluri, & R V prakash, "Creep damage characterisation using a low amplitude nonlinear ultrasonic technique", *Materials Characterization*, 2011; 62:275-286.

[11] D N Alleyne, & P Cawley, "The long range detection of corrosion in pipes using Lamb waves," *Rev. of Prog. In Quan. NDE*,1995; 14: 2075-2080.

[12] J L Rose, J Ditri, A Pilarski, K Rajana, & F T Carr., "A guided wave inspection technique for nuclear steam generator tubing", *NDT&E Int*.,1994; 27: 307-330.

[13] D J Roth, M J Verrilli, R E Martin, & L M Cosgriff, "Initial attempt to characterize oxidation damage in C/SiC composite using an ultrasonic guided wave method*", J. Am. Ceram. Soc.*, 2005; 88(8): 2164-2168.

[14] D J Roth, L M Cosgriff, R E Martin, M J Verrilli, & R T Bhatt, "Microstructural and defect characterization in ceramic composites using an ultrasonic guided wave scan system", 30th Annual Rev. of Quan. NDE, 2003; NASA/TM-2003-212518.

[15] J Y Kim, J Qu and L J Jacobs, "Experimental characterization of material nonlinearity using Lamb waves" *Appl. Phys. Lett.*, 2007; 90: 021901-1 – 021901-3.

[16] C Pruell, J Y Kim and L J Jacobs, "Evaluation of fatigue damage using nonlinear guided waves", *Smart Mater. Struct.*, 2009; 18: 035003-1 – 035003-7.

[17] C Pruell, J-Y. Kim, J Qu, and L J Jacobs, "A nonlinear-guided wave technique for evaluating plasticity- driven material damage in a metal plate", *NDT & E Int.*, 2009; 42: 199-203.

[18] ABAQUS, "Analysis User's Manual",6-9.2 ed., 2008.

[19] F Moser, L J Jacobs, J Qu, "Modeling elastic wave propagation in waveguides with the finite element method", *NDT & E Int.*, 1999; 32: 225-234.

[20] N P Yelve, M Mitra, P M Majumdar, "Higher harmonics induced in lamb wave due to

Distribution Code A: Approved for public release, distribution is unlimited.

partial debonding of piezoelectric wafer transducers", *NDT & E Int.,* 2014; 63: 21-27.

[21] C Pruell, J – Y Kim, J Qu, L Jacobs, "Evaluation of plasticity driven material damage using lamb waves", *Appl. Phys. Lett.,* 2007; 91: 231911 1-3.

[22] L H Taylor, F R Rollins Jr., "Ultrasonic study of three-phonon interactions. I. Theory", *The Phy. Rev.,* 1964; 136 (3A): A591 – A596.

[23] A Demcenko, R Akkerman, P B Nagy, R Loendersloot, "Noncollinear wave mixing for non-linear ultrasonic detection of physical ageing in PVC", *NDT & E Int.,* 2012; 49: 34-39.

[24] M Liu, G Tang, L J Jacobs, J Qu, "Measuring acoustic nonlinearity parameter using collinear wave mixing", *J. of Appl. Phy.*; 2012; 112: 024908-1 – 024908-6.

[25] M F Müller, J Y Kim, J Qu, and L J Jacobs, "Characteristics of second harmonic generation of Lamb waves in nonlinear elastic plates", *J. Acoust. Soc. Am.,* 127 (4), p. 2141-2152 (2010).

[26] J H Cantrell, and W T Yost, "Nonlinear acoustical assessment of precipitation nucleation and growth in aluminium alloy2024', *Review of progress in QNDE*, Vol. 15, 1347 (1999).

[27] D C Hurkey, D Balzar, and P T Purtscher, and K W Hollman, "Nonlinear ultrasonic parameter in quenched martensitic steel", *J Appl. Phys*., 83(9), 4584-4588 (1998).

[28] W L Morris, O Buck, and R V Inman, "Acoustic harmonic generation due to fatigue in high strength aluminium", *J. Appl. Phys*., 50(11), 6737-6741 (1979).

[29] P B Nagy, "Fatigue damage assessment by nonlinear ultrasonic materials characterization", *Ultrasonics*, 36; 375-381 (1998).

[30] K Y Jhang, and K C kim, "Evaluation of material degradation using nonlinear acoustic effect", *Ultrasonics*, 37; 39-44 (1999).

[31] J Hermann, J Y Kim, L J Jacobs, J Qu, J W Littles, and M F Savage, "Assessment of material damage in a nickel-base superalloy using nonlinear Rayleigh surface waves", *J. Appl. Phys.*, 99; 124913-1 – 124913-8 (2006).

[32] G Shui, J Y Kim, J Qu, Y S Wang, and L J Jacobs, "A new technique for measuring the acoustic nonlinearity of materials using Rayleigh waves", *NDT & E Int*., 41; 326-329 (2008).

[33] M Liu, J Y Kim, L J Jacobs, and J Qu, "Experimental study of nonlinear Rayleigh wave propagation in shot-peened aluminium plates- Feasibility of measuring residual stress", *NDT & E Int*., 44; 67-74 (2011).

[34] M Deng, and J Pei, "Assessment of accumulated fatigue damage in solid plates using nonlinear Lamb wave approach", *Appl. Phys. Lett*., 90; 121902 - (2007).

[35] A Metya, N Parida, D K Bhattacharya, N R Bandyopadhyay, and S Palit Sagar,

Distribution Code A: Approved for public release, distribution is unlimited.

"Assessment of localized plastic deformation during fatigue in polycrystalline copper by nonlinear ultrasonic", *Metall. and Mat. Trans. A*, 38A; 3087- 3092 (2007).

[36] C Bermes, J Y Kim, J Qu, and L J Jacobs, "Nonlinear Lamb waves for the detection of material nonlinearity", *Mech. Sys. and Sig. Process*., 22; 638-646 (2008).

[37] C Pruell, J Y kim, J Qu, and L J Jacobs, "Evaluation of fatigue damage using nonlinear guided waves", *Smart. Mat. and Struc.*, 18; 035003-035010 (2009).

[38] C Pruell, J Y Kim, J Qu, and L J Jacobs, "A nonlinear-guided wave technique for evaluating plasticity-driven material damage in a metal plate", *NDT & E Int*., 42; 199-203 (2009).

[39] K H Matlack, J Y Kim, L J Jacobs, J Qu, "Experimental characterization of efficient second harmonic generation of Lamb wave modes in a nonlinear elastic isotropic plate", *J. Appl. Phys.*, 109; 014905-1 – 014905-5 (2011).

[40] M Hong, Z Su, Q Wang, L Cheng, and X Qing, "Modeling nonlinearities of ultrasonic waves for fatigue damage characterization: Theory, simulation, and experimental validation", *Ultrasonics*, 54; 770-778 (2014).

[41] Y X Xiang, F Z Xuan, and M X Deng, "Evaluation of thermal degradation induced material damage using nonlinear Lamb waves", *Chin. Phys. Lett*., 27(1); 016202-1 – 016202-4 (2010).

[42] Y Xiang, M Deng, F Z Xuan, and C J Liu, "Cumulative second-harmonic analysis of ultrasonic Lamb waves for ageing behaviour study of modified-HP austenite steel", *Ultrasonics*, 51; 974-981 (2011).

[43] Y Xiang, M Deng, F Z Xuan, and C J Liu, "Effect of precipitate-dislocation interactions on generation of nonlinear Lamb waves in creep-damaged metallic alloys", *J. Appl. Phys.*, 111; 104905-1 – 104905-9 (2012).

[44] Y Xiang, M Deng, and F Z Xuan, "Creep damage characterization using nonlinear ultrasonic guided wave method: A mesoscale model", *J. Appl. Phys*., 115; 044914-1 – 044914-11 (2014).

[45] W J N de Lima, and M F Hamilton, "Finite-amplitude waves in isotropic elastic plates", *J. Sound and Vib*., 265; 819-839 (2003).

[46] C Bermes, J Y Kim, J Qu, and L J Jacobs, "Experimental characterization of material nonlinearity using Lamb waves", *Appl. Phys. Lett*., 90; 021901-1 – 021901-3 (2007).

[47] N Matsuda, and S Biwa, "Phase and group velocity matching for cumulative harmonic generation in Lamb waves", *J. Appl. Phys.*, 109; 094903-1 – 094903-11 (2011).

[48] A Hikata, B B Chick, and C Elbaum, "Dislocation contribution to the second harmonic generation of ultrasonic waves", *J. Appl. Phys.*, 36(1); 229-236 (1965).

Distribution Code A: Approved for public release, distribution is unlimited.

[49] A Hikata, C Elbaum, "Generation of ultrasonic second and third harmonics due to dislocations", Phys. Rev., 144; 469 (1966).

[50] W L Morris, O Buck, and R V Inman, "Acoustic harmonic generation due to fatigue damage in high strength aluminium", *J. Appl. Phys.*, 50 (11); 6737-6741 (1979).

[51] J H Cantrell, W T Yost, "Acoustic harmonic generation from fatigue induced dislocation dipoles", *Philos Mag A*, 69 (2); 315-326 (1994).

[52] W D Cash, and W Cai, "Dislocation contribution to acoustic nonlinearity: The effect of orientation dependent line energy", *J. Appl. Phys.*, 109; 014915-1 – 014915-10 (2011).

[53] N Mujica, M T Cerda, R Espinoza, J Lisoni, and F Lund, "Ultrasound as a probe of dislocation density in aluminium", *Acta Mater.*, 60; 5828-5837 (2012).

[54] F Lund, "Response of a stringlike dislocation loop to an external stress", *J. Mater. Res.*, 03(02); 280-297 (1988).

[55] K Maruyama, K Sawada, and J-i Koike, "Strengthening mechanism of creep resistant tempered martensitic steel," *ISIJ Int.*, 41(6); 641-653 (2001).

[56] C Panait, W Bendick, A Fuchsmann, A – F Gourgues-Lorenzon, and J Besson, "Study of the microstructure of the Grade 91 steel after more than 100,000h of creep exposure at 600^0C", Int. J. Of Press. Vess. And Pip., 87; 326-335 (2010).

[57] L Cipolla, S Caminda, D Venditti, H K Danielsen, and A Di Gianfrancesco, "Microstructural evolution of ASTM P91 after 100,000 hours exposure at 550^0C and 600^0C", *9th Liege Conf. on Mat. for Adv. Power Engg.*, 27th-29th Sept. 2010, Liege.

[58] C Zener, "Theory of growth of spherical precipitates from solid solution", *J. Appl. Phys.*, 20; 950-953(1949)

[59] P Šohaj, R Foret, "Microstructural stability of 316TI/P92 and 17242/P91 weld joints", *METAL 2011*, 18th – 20th May 2011, Brno, Czech Republic, EU.

[60] P J Ennis, A C Filemonowicz, "Recent advances in creep-resistant steels for power plant applications", *Sadhana*, 28(3 & 4); 709-730 (2003).

[61] H Kumar, J N Mahapatra, R K Roy, R J Joseyphus, and A Mitra, "Evaluation of tempering behaviour in modified 9Cr-1Mo steel by magnetic non-destructive technique", J. Of Mat. Process. Tech., 210; 669-674 (2010).

[62] J H Cantrell, and W T Yost, "Effect of precipitate coherency strains on acoustic harmonic generation", *J. Appl. Phys.*, 81(7); 2957-2962 (1997).

[63] G E Dieter, Mechanical Metallurgy, *McGraw-Hill Book Co.*, 1988

[64] J H Cantrell, and W T Yost, "Determination of precipitate nucleation and growth rates from ultrasonic harmonic generation", *Appl. Phys. Lett.*, 77(13); 1952-1954 (2000).

[65] A C Eringen, Mechanics of Continua, (Krieger, Huntington, NY, 1980); 219

Distribution Code A: Approved for public release, distribution is unlimited.